Shap. Mem. Superelasticity (2016) 2:239–246
DOI 10.1007/s40830-016-0067-y

SPECIAL ISSUE: SHAPE MEMORY AND SUPERELASTIC TECHNOLOGIES CONFERENCE 2015, INVITED PAPER

Improving of Mechanical and Shape-Memory Properties in Hyperbranched Epoxy Shape-Memory Polymers

David Santiago[1] · Albert Fabregat-Sanjuan[1] · Francesc Ferrando[1] · Silvia De la Flor[1]

Published online: 31 March 2016

Abstract A series of shape-memory epoxy polymers were synthesized using an aliphatic amine and two different commercial hyperbranched poly(ethyleneimine)s with different molecular weights as crosslinking agents. Thermal, mechanical, and shape-memory properties in materials modified with different hyperbranched polymers were analyzed and compared in order to establish the effect of the structure and the molecular weight of the hyperbranched polymers used. The presence of hyperbranched polymers led to more heterogeneous networks, and the crosslinking densities of which increase as the hyperbranched polymer content increases. The transition temperatures can be tailored from 56 to 117 °C depending on the molecular weight and content of the hyperbranched polymer. The mechanical properties showed excellent values in all formulations at room temperature and, specially, at $T_g^{E'}$ with stress at break as high as 15 MPa and strain at break as high as 60 %. The shape-memory performances revealed recovery ratios around 95 %, fixity ratios around 97 %, and shape-recovery velocities as high as 22 %/min. The results obtained in this study reveal that hyperbranched polymers with different molecular weights can be used to enhance the thermal and mechanical properties of epoxy-based SMPs while keeping excellent shape-memory properties.

This article is an invited paper selected from presentations at the International Conference on Shape Memory and Superelastic Technologies 2015, held May 18–22, 2015, in Chipping Norton, Oxfordshire, United Kingdom.

✉ Silvia De la Flor
silvia.delaflor@urv.net

[1] Department of Mechanical Engineering, Universitat Rovira i Virgili, Av. Països Catalans 26, 43007 Tarragona, Spain

Keywords Shape-memory · Epoxy · Hyperbranched · Mechanical properties · Smart materials

Introduction

Shape-memory polymers (SMPs) are a class of materials that can change their shape when an external stimulus is applied. These polymers can be processed to have a permanent shape by conventional techniques, and then deformed and fixed in a new or temporary shape that can remain stable until the stimulus is applied [1]. This shape changing is called the shape-memory effect (SME) and it is usually driven by heat. However, it can also be driven by light, a magnetic field, or an electrical current. These smart materials have attracted a lot of interest in recent years due to their wide range of applications including self-deployable structures for aerospace applications, biomedical devices, or smart fiber and fabrics [2–4].

The most common SMPs are thermoplastics because they are extremely ductile and easy to process [5, 6], and, therefore, suitable for a wide variety of potential applications. There are also some examples of SMP composites with improved mechanical performance [7, 8]. However, in recent years, a number of studies have reported shape-memory thermosets with excellent mechanical and shape-memory properties, such as epoxy-based or acrylate-based SMPs [9, 10].

Epoxy resins are widely used in many applications (coatings, adhesives, or matrices in composites) because of their chemical resistance, thermal stability, and good mechanical properties [11]. However, their brittle behavior and low elongation at break greatly limit their use as SMPs. Many studies have focused on overcoming this limitation by selecting suitable crosslinking agents which enhance

local mobility and deformability of the networks [12–15]. Although the toughness of epoxies is greatly improved in such networks, the mechanical properties in terms of tensile strength may remain a limitation. So new kinds of shape-memory epoxy polymer need to be found that combine high values of tensile strength and maximum deformation above and below the transition temperature for more mechanically demanding applications such as thermomechanical actuators.

Our research group recently reported the use of a low molecular weight hyperbranched polymer as crosslinking agent for epoxy-based SMPs [9]. The results revealed that the presence of hyperbranched polymer led to good thermal, mechanical, and shape-memory properties. These results indicate that other hyperbranched polymers should be used if shape-memory epoxy polymers are to be further improved. To this end, in this study, two hyperbranched polymers with different molecular weights have been used as crosslinking agents to determine the effect of the hyperbranched structure and molecular weight on the thermomechanical and shape-memory properties of epoxy-based SMPs.

Materials and Experimental Methods

Materials

Diglycidyl ether of bisphenol A (Araldite GY 240, Huntsman) with a weight per epoxy equivalent of 182 g/mol was used as the base epoxy resin (Fig. 1a). An aliphatic diamine (Jeffamine D400, Huntsman) with $M_w = 430$ g/mol (Fig. 1b) and two different commercial hyperbranched poly(ethyleneimine)s Lupasol® FG with $M_w = 800$ g/mol and Lupasol® PR8515 with $M_w = 2000$ g/mol (BASF) (Fig. 1c) were used as crosslinking agents.

Various formulations with different contents of diglycidyl ether of bisphenol A (DG), Jeffamine-D400 (D400), and Lupasol® FG (LP FG) or Lupasol® PR8515 (LP PR) were prepared (Table 1) as crosslinking agents. The proportions of reactants in each formulation were selected so that the molecular structure consisted of stoichiometric DG-D400 and DG-LP networks. The sample nomenclature X-Y-Z used in Table 1 indicates the weight fraction of stoichiometric DG-D400 (X) and DG-LP (Y) networks and the type of Lupasol® used (Z).

Thermomechanical Characterization

The thermomechanical properties were measured using a DMA Q800 (TA Instruments) equipped with a 3-point bending clamp. Prismatic rectangular samples of ca. 30 mm × 5.5 mm × 2.5 mm were analyzed at 1 Hz, 0.1 % strain, and a heating rate of 3 °C/min. The glass transition temperature was determined from the peak in tan δ. The values of storage modulus E' were evaluated below and above glass transition.

Mechanical Characterization

The mechanical properties at room temperature were evaluated using an electromechanical universal testing machine (Zwick 1445) with specially designed grips. The specimens were sized in accordance with ASTMD638 requirements and had a Type IV dog-bone shape. The experiments were performed at a crosshead speed of 1 mm/min.

The mechanical properties at $T_g^{E'}$ were measured using a DMA Q800 equipped with a film-tension clamp in force-controlled mode. Prismatic rectangular samples of ca. 20 mm × 2.5 mm × 0.5 mm were analyzed at $T_g^{E'}$ at a force rate of 1 N/min. In both cases, the stress–strain relationship was obtained using the specifications established in ASTMD638.

Shape-Memory Characterization

The shape-memory properties were measured using a DMA Q800 with a force-controlled mode and equipped with a film-tension clamp. Prismatic rectangular samples of ca. 20 mm × 2.5 mm × 0.5 mm were used in shape-memory performances. The method used to create a temporary shape and trigger the SME was a thermomechanical procedure called programming (Fig. 2). This programming consisted of four steps. (1) First the sample was heated to programming temperature T_{prog} and deformed to a prescribed value of maximum stress σ_m at 1 MPa/min. In this stage, the deformation of the sample was ε_m. (2) The next step was to cool the sample to below transition temperature T_{low} ($\sim$25 °C) so as to fix the temporary shape. (3) After fixation, the stress was released at the same stress rate of 1 MPa/min. Once the sample had been unloaded, the deformation of the sample was ε_u. (4) The SME was triggered by heating the sample to a recovery temperature $T_{recovery}$ ($T_g + 10$ °C) at a heating rate of 3 °C/min. The amount of non-recoverable deformation at the end of programming was ε_p.

The programming temperature was chosen as the onset of the glass transition temperature $T_g^{E'}$ of each sample. According to Yakacki et al., [16] a peak in the deformability of shape-memory acrylate-based polymers can be obtained at a temperature coinciding with the onset of glass transition temperature. Feldkamp and Rousseau [17] reported the same phenomenon in epoxy-based systems.

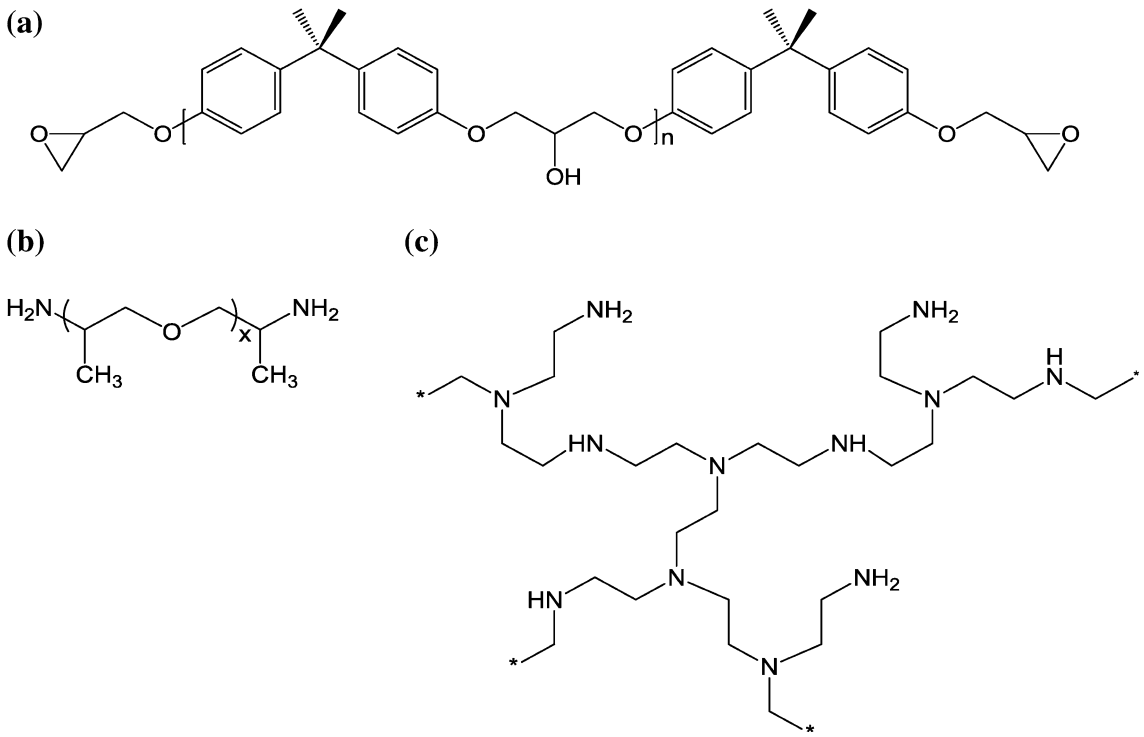

Fig. 1 **a** Chemical structure of DGEBA ($n = 0.08$); **b** chemical structure of Jeffamine D400 ($x = 6.1$); **c** chemical structure of Lupasol® FG

Table 1 Composition of the formulations studied

Sample	wt% DG	wt% D400	wt% Lupasol®	D400: LP amine ratio[a]	ν_c (mol/g)[b]
90-10-FG	63.5	34.8	1.7	4.010	0.001915
80-20-FG	65.7	31.0	3.3	1.782	0.002127
70-30-FG	67.9	27.1	5.0	1.040	0.002339
60-40-FG	70.2	23.2	6.6	0.668	0.002551
50-50-FG	72.4	19.4	8.3	0.446	0.002763
40-60-FG	74.6	15.5	9.9	0.297	0.002975
30-70-FG	76.8	11.6	11.6	0.191	0.003187
90-10-PR	63.4	34.8	1.8	3.771	0.00194
80-20-PR	65.5	31.0	3.5	1.676	0.002176
70-30-PR	67.6	27.1	5.3	0.978	0.002412
60-40-PR	69.8	23.2	7.0	0.629	0.002648
50-50-PR	71.9	19.4	8.8	0.419	0.002885
40-60-PR	74.0	15.5	10.5	0.279	0.003121
30-70-PR	76.1	11.6	12.3	0.180	0.003357

[a] Total primary, secondary, and tertiary amine groups present in the crosslinking agent

[b] υ_c is the crosslinking density, and it was calculated assuming that all amine groups turn into crosslinks

The most significant parameters for quantifying shape-memory properties are the shape-recovery ratio (R_r) and the shape-fixity ratio (R_f). The shape-recovery ratio (Eq. 1) quantifies the ability of the SMP to recover its original shape and was calculated as the total deformation recovered with respect to the maximum deformation reached during the programming. The shape-fixity ratio, calculated from Eq. (2), quantifies the ability of the SMP to fix the temporary shape. It was calculated as the deformation after the stress was released with respect to the maximum deformation.

$$R_r(\%) = \frac{\varepsilon_m - \varepsilon_p}{\varepsilon_m} \times 100, \quad (1)$$

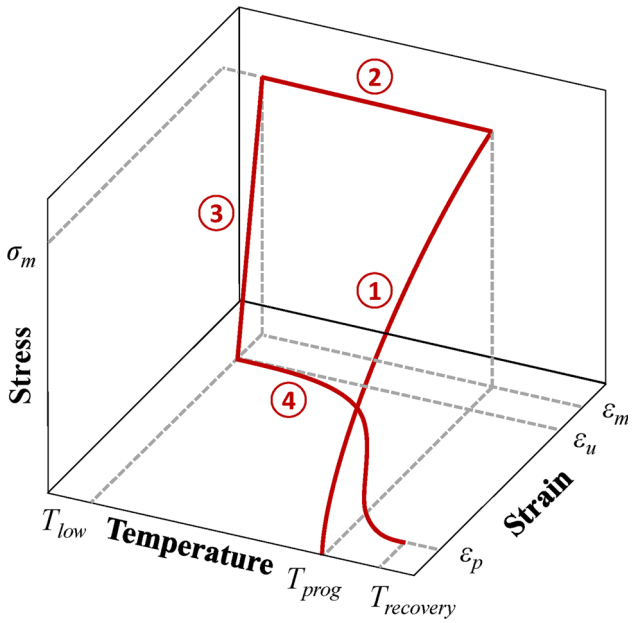

Fig. 2 Scheme of the thermomechanical programming

$$R_f(\%) = \frac{\varepsilon_u}{\varepsilon_m} \times 100. \quad (2)$$

Another parameter of interest in evaluating shape-memory ability is the shape-recovery rate (V_r). This quantifies the velocity at which the permanent shape is recovered and it is calculated according to Eq. 3:

$$V_r\left(\%/\text{min}\right) = \frac{\left(\frac{\varepsilon_{rec,15\%} - \varepsilon_{rec,85\%}}{\varepsilon_{rec,15\%}}\right) \times 100}{\Delta t_{15-85\%}}, \quad (3)$$

where $\varepsilon_{rec,15\ \%}$ is the deformation corresponding to a shape recovery of 15 %, $\varepsilon_{rec,85\ \%}$ is the deformation corresponding to a shape recovery of 85 %, and $\Delta t_{15-85\ \%}$ is the time interval between these two points. The difference between deformations corresponding to a shape recovery of 15 and 85 %, $\varepsilon_{rec,15\ \%}$–$\varepsilon_{rec,85\ \%}$, was calculated with respect to $\varepsilon_{rec,15\ \%}$ in order to avoid the influence of the maximum deformation on V_r.

Results and Discussion

Thermomechanical Properties

The thermomechanical properties of formulations with Lupasol® FG and Lupasol® PR8515 are listed in Table 2. The glass transition temperatures of these materials can be controlled by varying the chemical composition of the formulations. T_gs show values between 60 and 117 °C with LP FG and 56 and 112 °C with LP PR. Formulations with LP PR have slightly lower T_gs than formulations with LP FG. The higher molecular weight of Lupasol® PR8515 results in longer branches than Lupasol® FG, and these longer branches improve the molecular motion of the network in comparison with formulations with the lower molecular weight counterpart. Accordingly, these materials can be used in shape-memory applications that require a broad range of transition temperatures.

A higher content of Lupasol® means that the crosslinking density is also higher (Table 1) because of the higher number of reactive amine groups per unit mass and the presence of internal branching points. This decreases the average chain length between netpoints and restricts the molecular mobility, which leads to an increase in T_g. As can be observed in Table 2, an increase in Lupasol® also lowers and broadens the curve of tan δ. The shape of the tan δ curve can be correlated with its network structure: the higher and narrower the shape of the curve of tan δ, the more homogeneous and mobile the network structure is [18]. The presence of Lupasol® leads to a more heterogeneous network structure due to the inherently disperse nature of the hyperbranched poly(ethyleneimine) and the presence of different types of crosslinks from the pre-existing tertiary amines and the reacted primary and secondary amines. The longer branches of LP PR, which decrease the transition temperature in comparison with formulations with LP FG, increase the heterogeneity and dispersity of the networks, which have lower and wider curves of tan δ (Table 2).

All formulations show very high values of storage modulus in the glassy region around 3 GPa, which is higher than most of the shape-memory epoxy resins found in the literature [13–15]. The storage modulus in the rubbery region E'_r increases from 16 MPa to 52 MPa as the LP FG content increases and from 15 to 58 MPa as the LP PR content increases. According to the theory of rubber elasticity, E'_r is roughly proportional to the crosslinking density and the rubbery modulus (Table 2) is expected to increase with the crosslinking density. Given the hyperbranched structure of Lupasol®, which has a considerable number of internal branching points and very short ethylene segments within, unlike the long, and flexible aliphatic structure of Jeffamine D400, mobility can be expected to be restricted and deformability lower when the Lupasol® content is increased in the cured thermosets.

Mechanical Properties

Most of the articles about SMPs found in the literature focus on mechanical properties at high temperature so that deformations can be high during the programing of the temporary shape. However, the characterization of the mechanical properties at room temperature is important for applications such as thermomechanical actuators, which

Table 2 Thermomechanical data obtained by DMA: glass transition temperature (T_g), onset temperature of the glass transition temperature ($T_g^{E'}$), storage modulus in glassy, and rubbery regions (E'_g and E'_r respectively)

Sample	T_g[a] (°C)	$T_g^{E'}$ (°C)	tan δ peak	FWHM[b] (°C)	tan δ area[c] (°C)	E'_g[d] (MPa)	E'_r[e] (MPa)	E'_g/E'_r
90-10-FG	60	50	0.96	15	14.83	2878	16	183
80-20-FG	68	57	0.82	18	14.61	2880	17	166
70-30-FG	77	63	0.71	20	14.41	3105	23	137
60-40-FG	87	71	0.62	21	13.09	3149	29	110
50-50-FG	96	80	0.54	23	12.60	3110	34	91
40-60-FG	104	88	0.50	24	11.83	3221	41	79
30-70-FG	117	98	0.41	25	10.08	2858	52	55
90-10-PR	56	48	0.98	15	15.11	3050	15	198
80-20-PR	64	55	0.78	20	15.25	3111	18	172
70-30-PR	70	60	0.62	25	15.26	3253	22	150
60-40-PR	79	65	0.57	27	15.59	3008	23	128
50-50-PR	89	73	0.50	29	14.58	3166	32	98
40-60-PR	99	78	0.38	33	12.60	2936	44	67
30-70-PR	112	89	0.34	34	11.50	2871	58	49

[a] Measured as the peak of tan δ

[b] Full width at half maximum

[c] Determined as the product of tan δ peak and FWHM

[d] Measured at T_g −40 °C

[e] Measured at T_g +40 °C

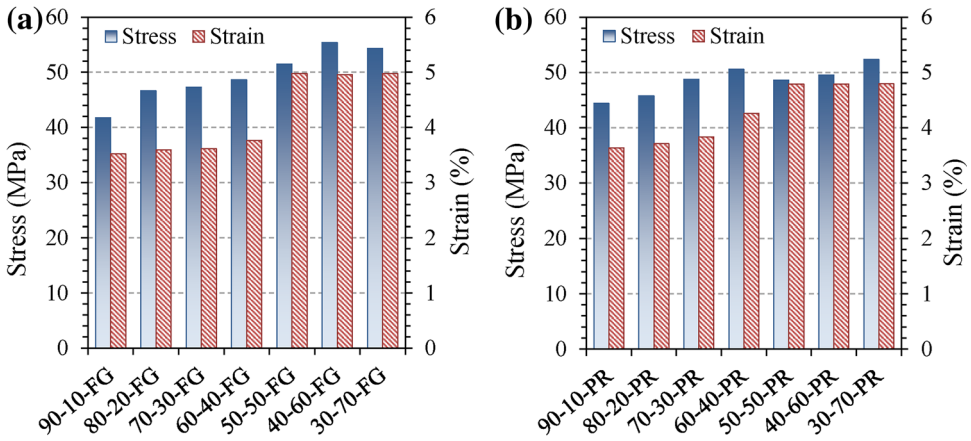

Fig. 3 Stress at break and strain at break of formulations with Lupasol® FG (**a**) and Lupasol® PR8515 (**b**) evaluated at T_{room}

must perform recovery stress or work against an external load. Figure 3 shows the values of stress at break and strain at break of formulations with Lupasol® FG (Fig. 3a) and with Lupasol® PR8515 (Fig. 3b) evaluated at T_{room}.

Both the stress at break and the deformation at break increase from 42 to 55 MPa and from 3.5 % to nearly 5.0 % with LP FG and from 44 to 52 MPa and from 3.7 to 4.8 % with LP PR. The observed tendency for stress at break values clearly shows that strength increases almost linearly with increasing crosslinking density and T_g in both formulations with LP FG and LP PR. The strain at break does not seem to be affected differently by crosslinking density in formulations with LP FG. Two distinctive regions are observed: from 90-10-FG to 60-20-FG, with values of strain at break around 3.6 %, and from 50-50-FG to 30-70-FG, with values of strain at break around 5 %. In formulations with LP PR, the strain at break increases linearly from 3.6 % in formulation 90-10-PR to 5.0 % in formulation 50-50-PR. From this point, the strain at break shows values around 5.0 % in the other formulations. These results suggest that the increase in the strain at break seems to be possible up to a certain value when the increasing crosslinking density limits the deformability of the network.

Properties below the T_g depend on a combination of factors such as cohesive forces and the presence of local mobility. Strain and stress at break increase with increasing T_g and depend mainly on the difference between the test temperature and T_g. It should be taken into account that when the Lupasol® content is increased, the DG content also increases (Table 1), which increases the number of hydroxyl groups from the epoxy-amine condensation and contributes to the cohesion of the network structure. The internal flexible structure of Lupasol®, which has limited local mobility below the glass transition temperature, may contribute to the observed behavior.

Figure 4 shows the values of stress at break and strain at break of formulations with LP FG (Fig. 4a) and with LP PR (Fig. 4b) at $T_g^{E'}$. All formulations show very high values of stress at break, above 10 MPa in all cases and up to 15 MPa in formulation 30-70-FG. Several studies have reported shape-memory epoxy networks with very high deformations at break at $T_g^{E'}$. However, the values of stress at break at $T_g^{E'}$ in shape-memory epoxy networks are usually lower than those reported in this paper [14, 17, 19].

The values of stress at break and strain at break have a more rigid structure as Lupasol® content increases, which means that strain at break decreases from 58 to 17 % in formulations with LP FG and from 50 to 13 % in formulations with LP PR. In general, an increase in the crosslinking density results in a less mobile and ductile network. On the macroscopic scale this leads to a lower failure strain and a higher stress at break. These results can be explained by the internal hyperbranched structure of Lupasol® which has short ethylene segments within and is less deformable than the long, flexible Jeffamine D400 structure.

Overall, for both temperatures, formulations with LP PR have values of stress at break and strain at break that are slightly lower than formulations with LP FG. These differences may be caused by the higher crosslinking density of formulations with LP PR and the presence of possible molecular interactions due to the longer branches of LP PR.

Shape-Memory Properties

To make a comparative study with the same level of load, every sample was stretched during the programming to a prescribed maximum stress (σ_m) that was 75 % of the stress at break ($\sigma_m = 0.75\sigma_b$).

Figure 5 shows the shape-recovery ratio and the shape-fixity ratio of formulations with Lupasol® FG (Fig. 5a) and with Lupasol® PR8515 (Fig. 5b). The average shape-recovery ratio and shape-fixity ratio over three cycles were calculated when programming under these conditions (σ_m and $T_g^{E'}$). All formulations show shape-recovery ratio values above 93 % and shape-fixity ratio values around 97 %, which demonstrates the excellent shape-memory properties of materials with both Lupasol® FG and Lupasol® PR8515.

The shape-recovery ratio decreases slightly as the Lupasol® content increases in both groups of formulations: from 96.3 % to 93.4 % with LP FG and from 96.5 to 92.9 % with LP PR. The maximum is for formulations 80-20-FG and 80-20-PR with $R_r = 97.4$ % and $R_r = 97.5$ %, respectively. The shape-fixity ratio is high with both types of Lupasol® and ranges from 98 to 94 % as the Lupasol® content increases.

These results can be correlated with thermomechanical properties and network structure. Formulations with a higher Lupasol® content have broader network relaxation because of the more heterogeneous network structure (Table 2) so it is more difficult to release the stored imposed stresses (step 1 in Fig. 2) during the recovery process. This decreases the shape-recovery ratio R_r. The local deformation of the internal structure of Lupasol® in the network, which has short ethylene segments within, has a lower contribution to conformational, entropic deformation than

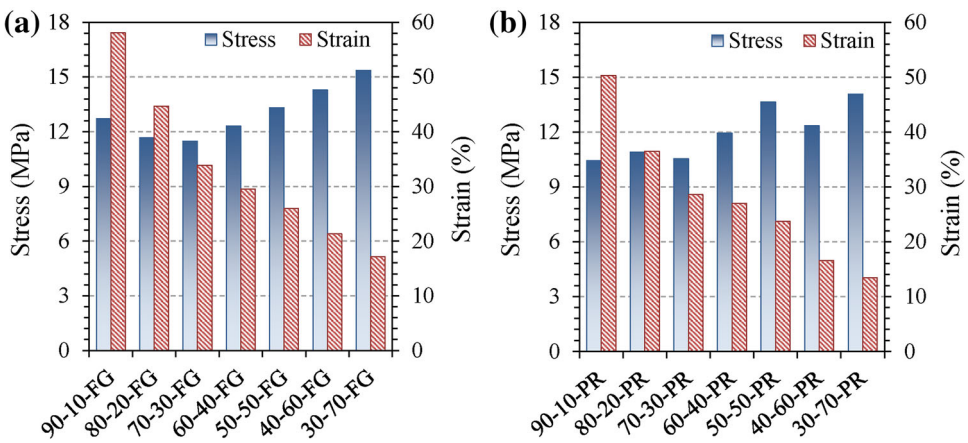

Fig. 4 Stress at break and strain at break of formulations with Lupasol® FG (**a**) and Lupasol® PR8515 (**b**) evaluated at $T_g^{E'}$

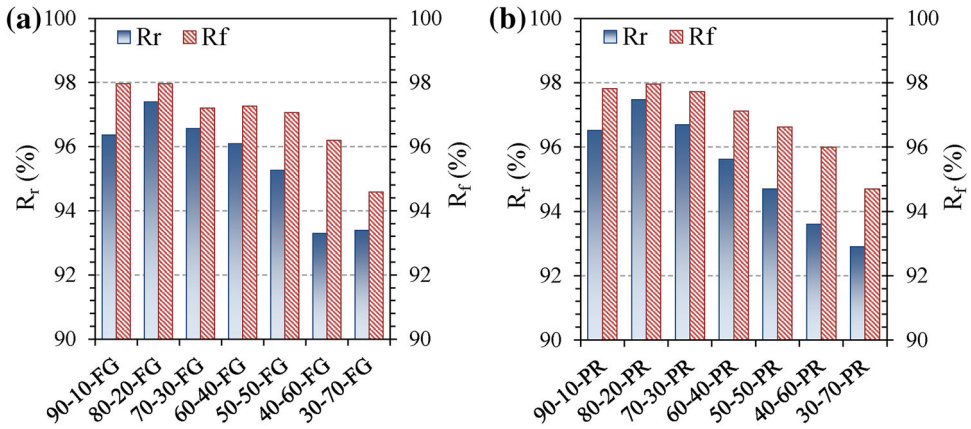

Fig. 5 Shape-recovery ratio (R_r) and shape-fixity ratio (R_f) of formulations with Lupasol® FG and (**a**) and with Lupasol® PR8515 (**b**)

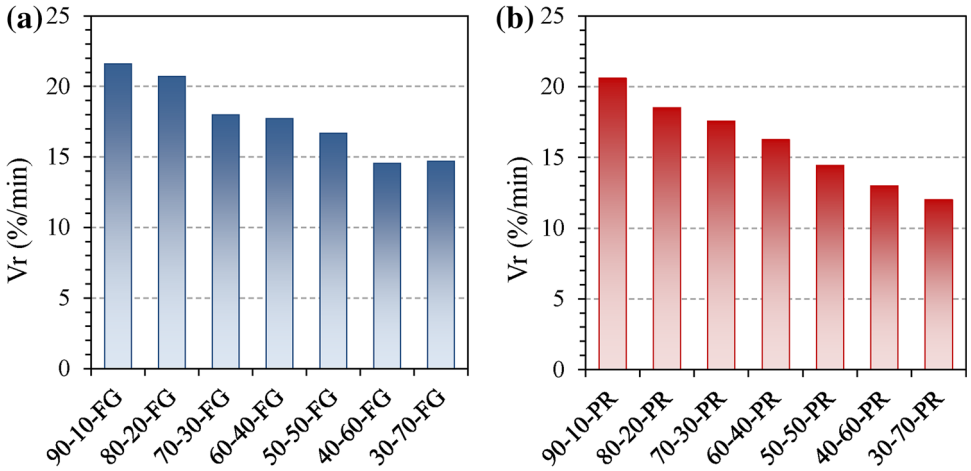

Fig. 6 Shape-recovery velocity (V_r) of formulations with Lupasol® FG (**a**) and with Lupasol® PR8515 (**b**)

longer D400 chains and can therefore relax immediately after stress release. A higher amount of spontaneous elastic recovery may be expected when formulations with a higher Lupasol® content are unloaded. In this case, shape-fixity ratios R_f are lower.

As mentioned above, LP PR has longer branches than LP FG. This means that formulations with LP PR have a more heterogeneous structure than formulations with LP FG and have slightly lower values of R_r and R_f.

Figure 6 shows the shape-recovery velocity V_r of formulations with Lupasol® FG (Fig. 6a) and Lupasol® PR8515 (Fig. 6b). It is observed that V_r decreases as the Lupasol® content increases. Formulations with a higher Lupasol® content have broader network relaxation because of the more heterogeneous network structure which hinders the recovery process. Thus, it takes longer to release the stored internal stresses during the recovery process in materials with a higher Lupasol® content. Formulations with LP PR have lower values of V_r due to the more heterogeneous networks than formulations with LP FG (see "Thermomechanical properties" section).

Conclusions

A series of shape-memory epoxy polymers was synthesized using an aliphatic amine and two commercial hyperbranched poly(ethyleneimine)s with different molecular weights as crosslinking agents. The influence of the structure of the hyperbranched polymers on the thermal, mechanical, and shape-memory properties was analyzed and discussed.

The thermomechanical measurements showed that an increase in the Lupasol® content led to more heterogeneous networks with higher crosslinking densities and higher T_gs. Formulations with Lupasol® PR8515 had lower T_gs but wider transitions than formulations with Lupasol® FG.

The tensile tests at room temperature showed that an increase in the Lupasol® content resulted in an increase in the stress at break and deformation at break, showing values around 55 MPa and 5 % in both groups of formulations. At the programming temperature $T_g^{E'}$, the stress at break showed excellent values above 10 MPa in all formulations and up to 15 MPa and deformations at break of

almost 60 %. The higher crosslinking density and the presence of possible molecular interactions of formulations with Lupasol® PR8515 resulted in slightly lower values of stress at break and strain at break than formulations with Lupasol® FG.

Shape-memory performances showed high values of shape-recovery, shape-fixity ratios, and shape-recovery velocity. The shape-memory properties were reduced when the Lupasol® content was increased because it restricted chain-conformational changes during deformation and molecular dynamics, which hindered the recovery and fixity processes and decreased the recovery velocity. Formulations with Lupasol® PR8515 presented slightly lower shape-memory properties because they were more heterogeneously structured than formulations with Lupasol® FG.

The results obtained show that hyperbranched polymers can be used as crosslinking agents for epoxy-based SMPs. The hyperbranched polymer content and molecular weight should be controlled. While materials with low molecular weight hyperbranched polymers showed slightly better mechanical and shape-memory properties, materials with higher molecular weight hyperbranched polymers had lower transition temperatures. Other mechanical properties can be analyzed in future work to determine the effect of both types of hyperbranched poly(ethyleneimine)s.

Acknowledgments The authors would like to thank MICINN (MAT2014-53706-C03-01) and the Generalitat de Catalunya (2014-SGR-67) for giving financial support.

References

1. Lendlein A, Kelch S (2002) Shape-memory polymers. Angew Chem Int Ed 41(12):2034–2057
2. Liu Y, Du H, Liu L, Leng J (2014) Shape memory polymers and their composites in aerospace applications: a review. Smart Mater Struct 23(2):023001
3. Cha KJ, Lih E, Choi J, Joung YK, Ahn DJ, Han DK (2014) Shape-memory effect by specific biodegradable polymer blending for biomedical applications. Macromol Biosci 14(5):667–678
4. Han HR, Chung SE, Park CH (2013) Shape memory and breathable waterproof properties of polyurethane nanowebs. Text Res J 83(1):76–82
5. Santiago D, Ferrando F, De La Flor S (2014) Effect of different shape-memory processing methods on the thermomechanical cyclic properties of a shape-memory polyurethane. J Mater Eng Perform 23(7):2561–2566
6. Santiago D, Ferrando F, De La Flor S (2014) Influence of holding time on shape recovery in a polyurethane shape-memory polymer. J Mater Eng Perform 23(7):2567–2573
7. Ohki T, Ni Q-Q, Ohsako N, Iwamoto M (2004) Mechanical and shape memory behavior of composites with shape memory polymer. Compos Part Appl Sci Manuf 35(9):1065–1073
8. Lu H, Yu K, Sun S, Liu Y, Leng J (2010) Mechanical and shape-memory behavior of shape-memory polymer composites with hybrid fillers. Polym Int 59(6):766–771
9. Santiago, D, Fernández-Francos, X, Ferrando F, De la Flor S (2015) Shape-memory effect in hyperbranched poly(ethyleneimine)-modified epoxy thermosets. J Polym Sci Part B Polym Phys 53(13):924–933
10. Santiago D, De la Flor S, Ferrando F, Ramis X, Sangermano M (2015) Thermomechanical properties and shape-memory behavior of bisphenol a diacrylate-based shape-memory polymers. Macromol Chem Phys. doi:10.1002/macp.201500261
11. Kumar KSS, Biju R, Nair CPR (2012) Progress in shape memory epoxy resins. React Funct Polym 73(2):421–430
12. Xie T, Rousseau IA (2009) Facile tailoring of thermal transition temperatures of epoxy shape memory polymers. Polymer 50(8):1852–1856
13. Leonardi AB, Fasce LA, Zucchi IA, Hoppe CE, Soulé ER, Pérez CJ, Williams RJJ (2011) Shape memory epoxies based on networks with chemical and physical crosslinks. Eur Polym J 47(3):362–369
14. Feldkamp DM, Rousseau IA (2011) Effect of chemical composition on the deformability of shape-memory epoxies. Macromol Mater Eng 296(12):1128–1141
15. Fan M, Liu J, Li X, Zhang J, Cheng J (2014) Thermal, mechanical and shape memory properties of an intrinsically toughened epoxy/anhydride system. J Polym Res 21(3):376
16. Yakacki CM, Willis S, Luders C, Gall K (2008) Deformation limits in shape-memory polymers. Adv Eng Mater 10(1–2):112–119
17. Feldkamp DM, Rousseau IA (2010) Effect of the deformation temperature on the shape-memory behavior of epoxy networks. Macromol Mater Eng 295(8):726–734
18. Wu XL, Kang SF, Xu XJ, Xiao F, Ge XL (2014) Effect of the crosslinking density and programming temperature on the shape fixity and shape recovery in epoxy-anhydride shape-memory polymers. J Appl Polym Sci 131(15):40559
19. Fan M, Yu H, Li X, Cheng J, Zhang J (2013) Thermomechanical and shape-memory properties of epoxy-based shape-memory polymer using diglycidyl ether of ethoxylated bisphenol-A. Smart Mater Struct 22(5):055034